Supporting Information for

Charge-State Control of Mn^{2+} Spin Relaxation Dynamics in Colloidal *n*-type $Zn_{1-x}Mn_xO$ Nanocrystals

Alina M. Schimpf, Jeffrey D. Rinehart,[†] Stefan T. Ochsenbein,[††] and Daniel R. Gamelin[*]

Department of Chemistry, University of Washington, Seattle, WA 98195-1700, USA
**Electronic address: Gamelin@chem.washington.edu*
[†]Present address: Department of Chemistry and Biochemistry, University of California in San Diego, La Jolla, CA 92013, USA
[††]Present address: Laboratory for Neutron Scattering and Imaging, Paul Scherrer Institut, CH-5232 Villigen PSI, Switzerland

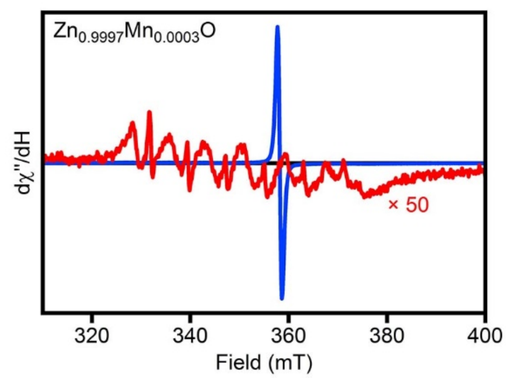

Figure S1. Room-temperature X-band CW EPR spectra of as-prepared (red) and maximally reduced (blue) colloidal d = 3.7 nm $Zn_{0.9997}Mn_{0.0003}O$ nanocrystals.

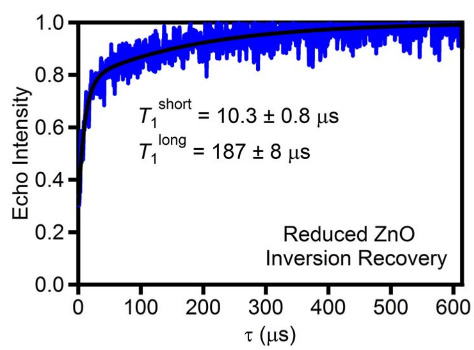

Figure S2. 4.5 K inversion recovery measured on photochemically reduced ($\langle n \rangle \sim 1$) ZnO nanocrystals. Data were fit to equation S1 and the short component (~67% of total amplitude) was used for T_1^e. Even though T_1^e likely decreases with increasing $\langle n \rangle$, this value of T_1^e (or k_{eSLR}) was used in the model calculations for all nanocrystal reduction levels (*i.e.*, for all n_e). Because the model already overestimates the decrease in T_1^{Mn} at $n_e > 1$, this approximation is not the source of the disagreement between model and experiment in Figure 4 of the main text.

$$I(\tau) = 1 - A_{\text{short}} \exp\left(-\tau / T_1^{\text{short}}\right) - A_{\text{long}} \exp\left(-\tau / T_1^{\text{long}}\right) \tag{S1}$$

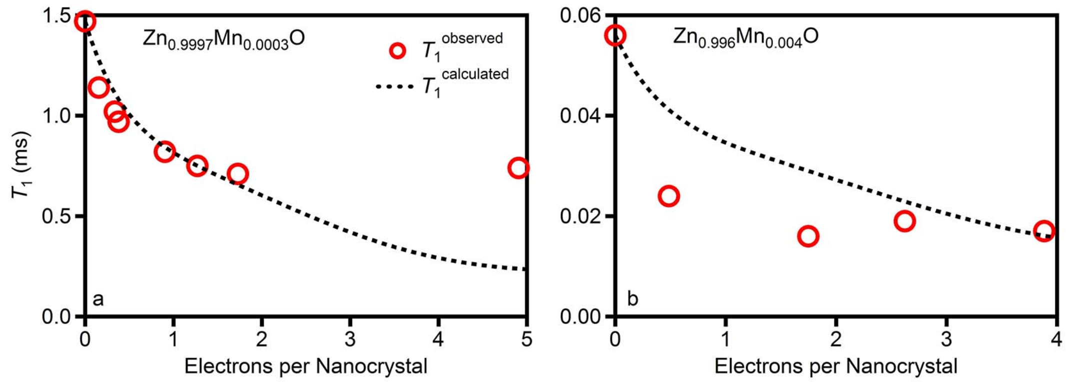

Figure S3. Experimental (circles) and calculated (dashed line) T_1 values plotted versus the average number of conduction-band electrons for (a) d = 3.7 nm $Zn_{0.9997}Mn_{0.0003}O$ and (b) d = 3.7 nm $Zn_{0.996}Mn_{0.004}O$ nanocrystals. Calculated values were obtained using equation S2 with $T_1^{\text{Mn}} = T_1^{\text{as-prepared}}$ and T_1^{e} = 10 μs. This model explicitly accounts for low- and intermediate-spin configurations expected from an orbital filling scheme. These calculations are intended for illustration purposes only, and it is unknown whether such low- and intermediate-spin configurations actually occur.

$$T_1^{\text{observed}} = \sum_{n_e=0}^{1} \frac{P(n_e)}{k_{\text{MnSLR}} + n_e k_{\text{eSLR}}} + \sum_{n_e=2}^{5} \frac{P(n_e)}{k_{\text{MnSLR}} + (n_e - 2) k_{\text{eSLR}}} + \sum_{n_e=6}^{7} \frac{P(n_e)}{k_{\text{MnSLR}} + (8 - n_e) k_{\text{eSLR}}} + \sum_{n_e=8}^{10} \frac{P(n_e)}{k_{\text{MnSLR}} + (n_e - 8) k_{\text{eSLR}}} \tag{S2a}$$

$$P(n_e) = \frac{\langle n \rangle^{n_e} e^{-\langle n \rangle}}{n_e!} \tag{S2b}$$